

Detector needs for photoelectron spectroscopy, diffraction, and holography, x-ray fluorescence holography, soft x-ray absorption/emission

--Or how to stop wasting photons

Chuck Fadley (UCD, LBNL) + H. Spieler, Z. Hussain (LBNL),
A. Nilsson (SLAC, Uppsala), B. Sinkovic (U.Conn.)

• Overview:

- Photoelectron spectroscopy, diffraction, holography:

- The experiments--core and valence spectra, energy and angle distributions, time resolution
- The present status:

1D (channeltrons or microchannel plates (MCPs))

2D (MCP+resistive anodes or MCP+ phosphor+CCD or MCP+collectors+ ASICs)

Capabilities and limitations--an example MCP+phosphor+CCD system

– A 1D demonstration project at LBNL: 1D, goal--768 channels, 50 μ , 1.0 MHz/channel, 1.0 GHz overall

– Future needs:

Dispersive analysis:

1D: 500-1000 channels, 20-50 μ pitch, 1 MHz/channel, 10-20 mm x 40 mm, 1 GHz overall

2D: 500-1000 (in E_k) x 500 (in k_x or x) = 250,000-500,000 pixels, ~40 μ x ~80 μ , 5G kHz-1 MHz/pixel,
~40 mm x ~40 mm, 1-100 GHz overall,

Time-of-flight analysis: time resolution from ~30 psec (present ALS bunch length) down to ~250 fs (LCLS)

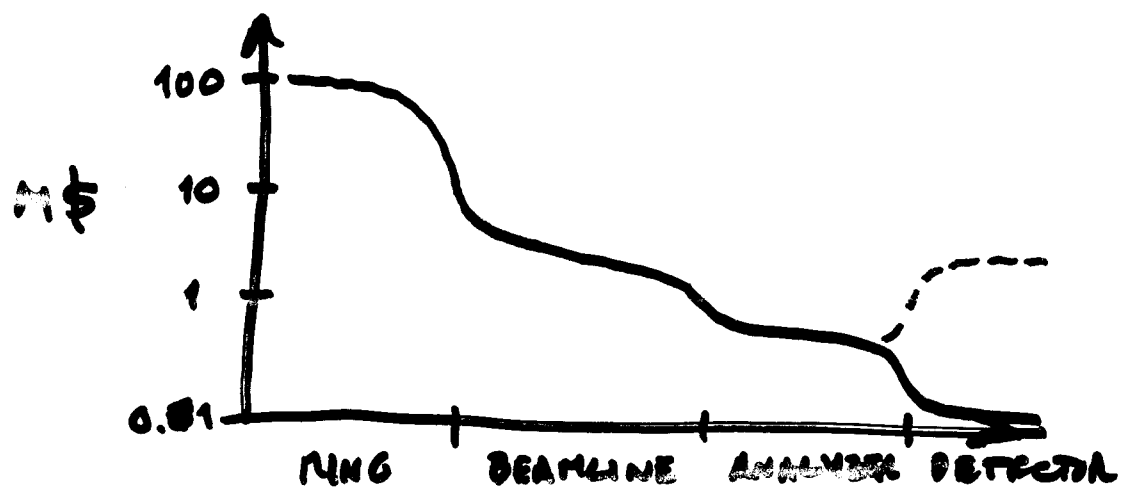
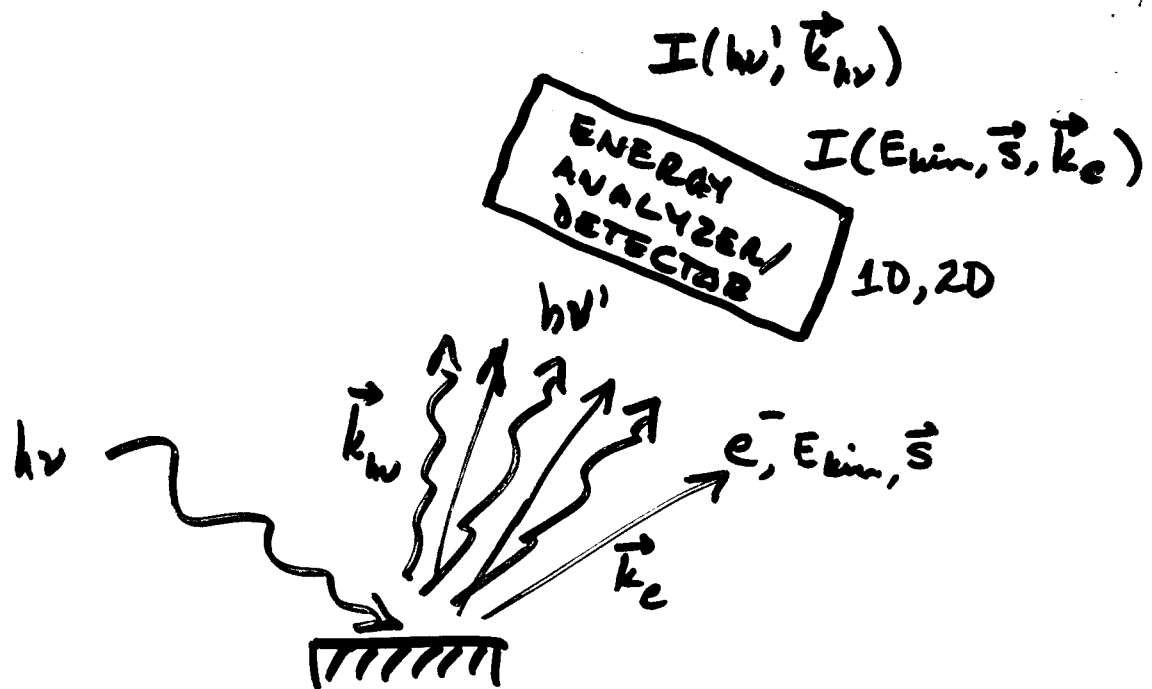
Spin detection: beyond microMott (10^{-3} - 10^{-4} efficiency)? a spatially resolved spin filter? (Siegmann et al., Sinkovic, Hulbert, Wu, Hussain)

- X-ray fluorescence holography:

- The experiments--direct and inverse holography
- The present status: Ge detectors up to 1 MHz over 4 elements (LBNL--Bucher, Fabris, et al.) or graphite crystal plus avalanche photodiode (ESRF--Marchesini et al.)
- Future needs-- ~1° angular resolution, ~100 eV resolution for x-rays at 6-20 keV, ~hemisphere coverage, 1-10 GHz overall→hologram in 1-10 sec

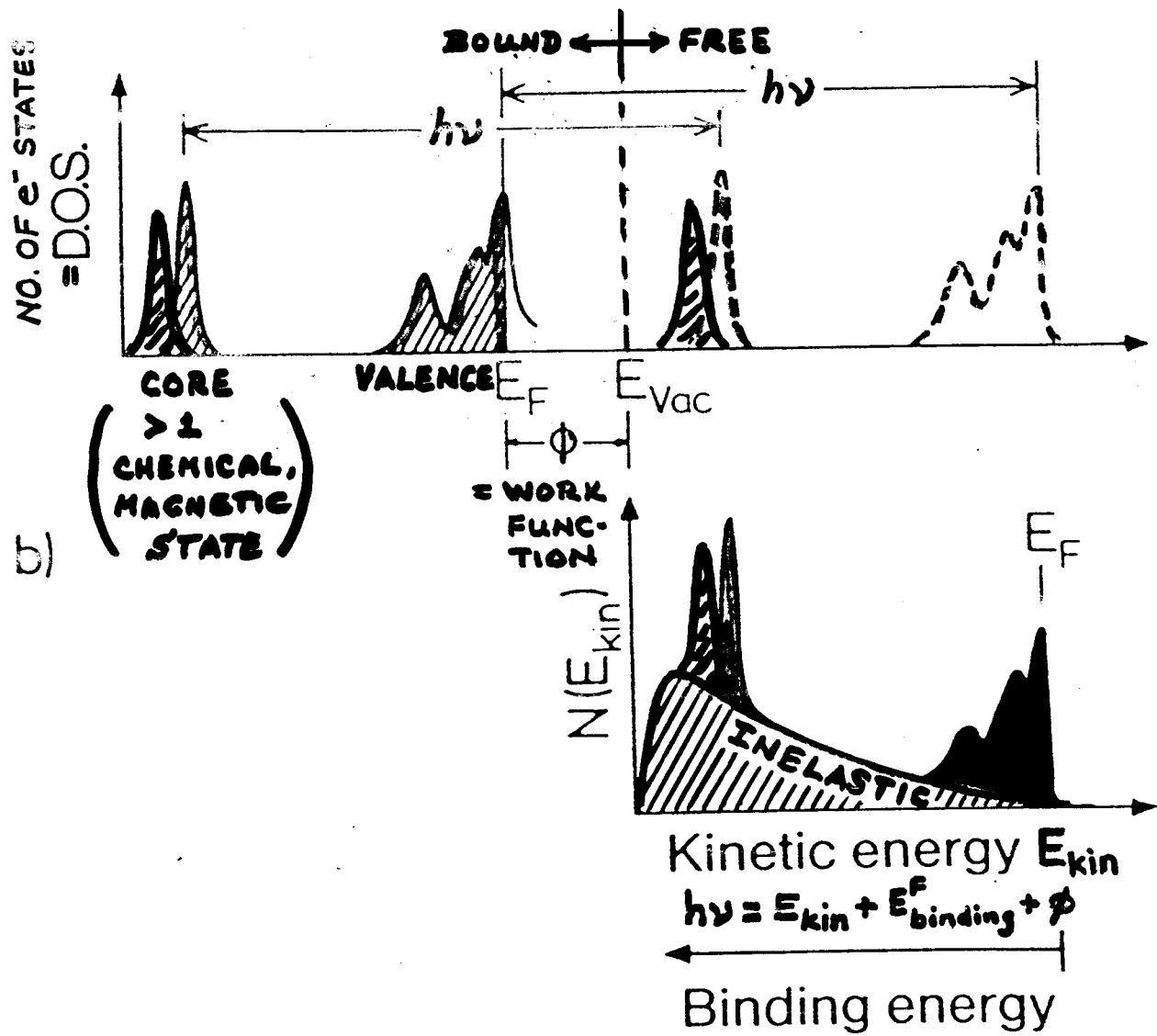
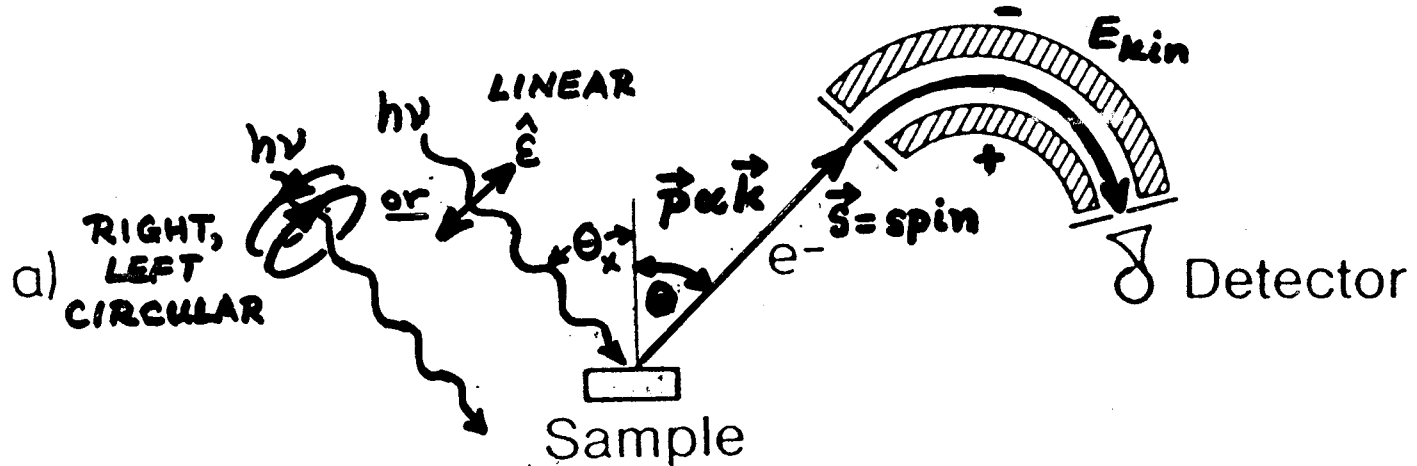
- Soft x-ray absorption spectroscopy:

- CCD detector with ~1 μ x ~1 μ resolution, overall 40 mm x 40 mm, low dark current
- Soft -ray emission spectroscopy, inelastic/elastic x-ray scattering:
 - 1:10⁴ energy resolution for 50-1500 eV, high throughput, 10-100x current best (Callcott et al.; Underwood et al.)--Not a "detector"?
- Some guidelines for the future:
 - Teams of scientists, postdocs, students with engineers, technicians, not one or the other
 - Sufficient funding to keep attention of participants, keep project moving along
 - Variety of approaches, from evolutionary building on existing technology (quicker payoff) to revolutionary (longer term)

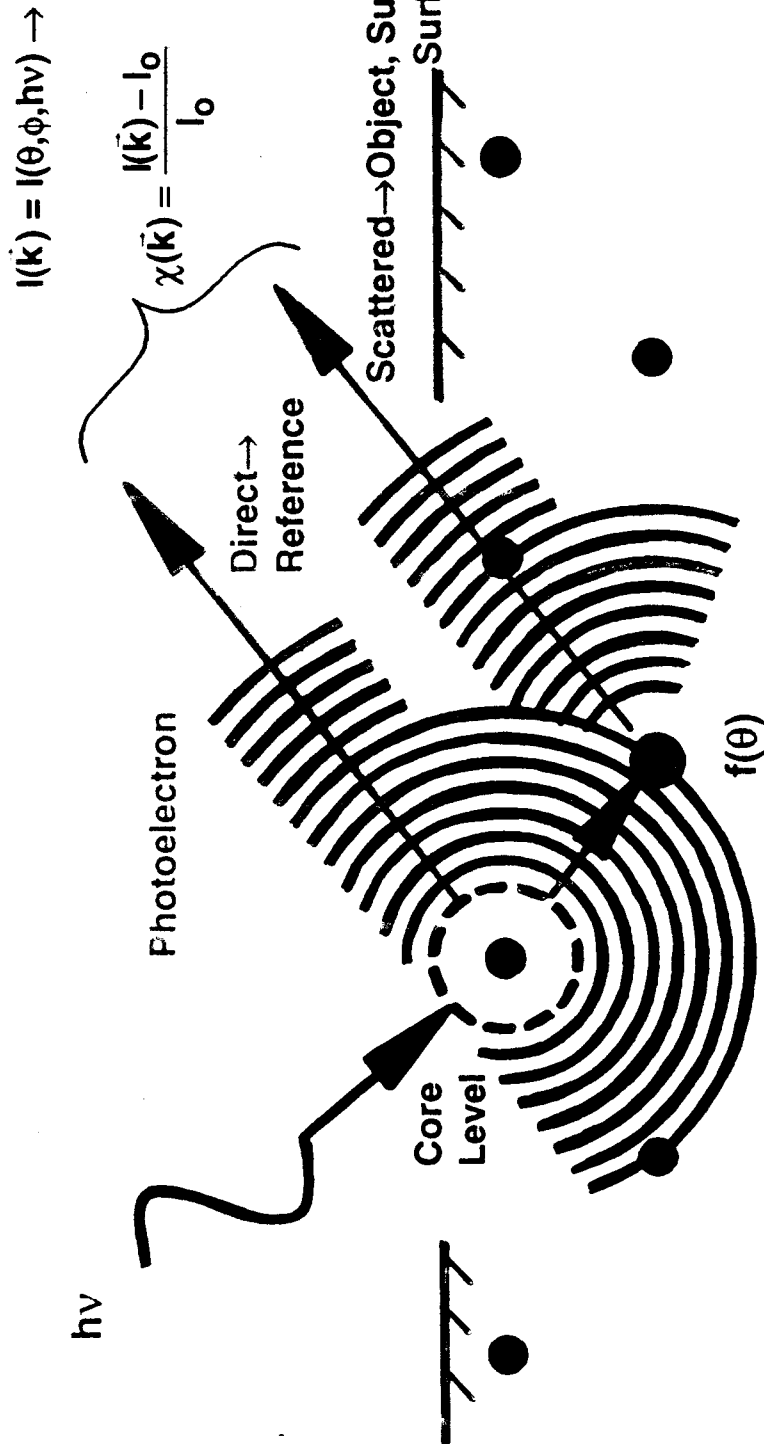


PHOTOELECTRON SPECTROSCOPY

Energy analyzer

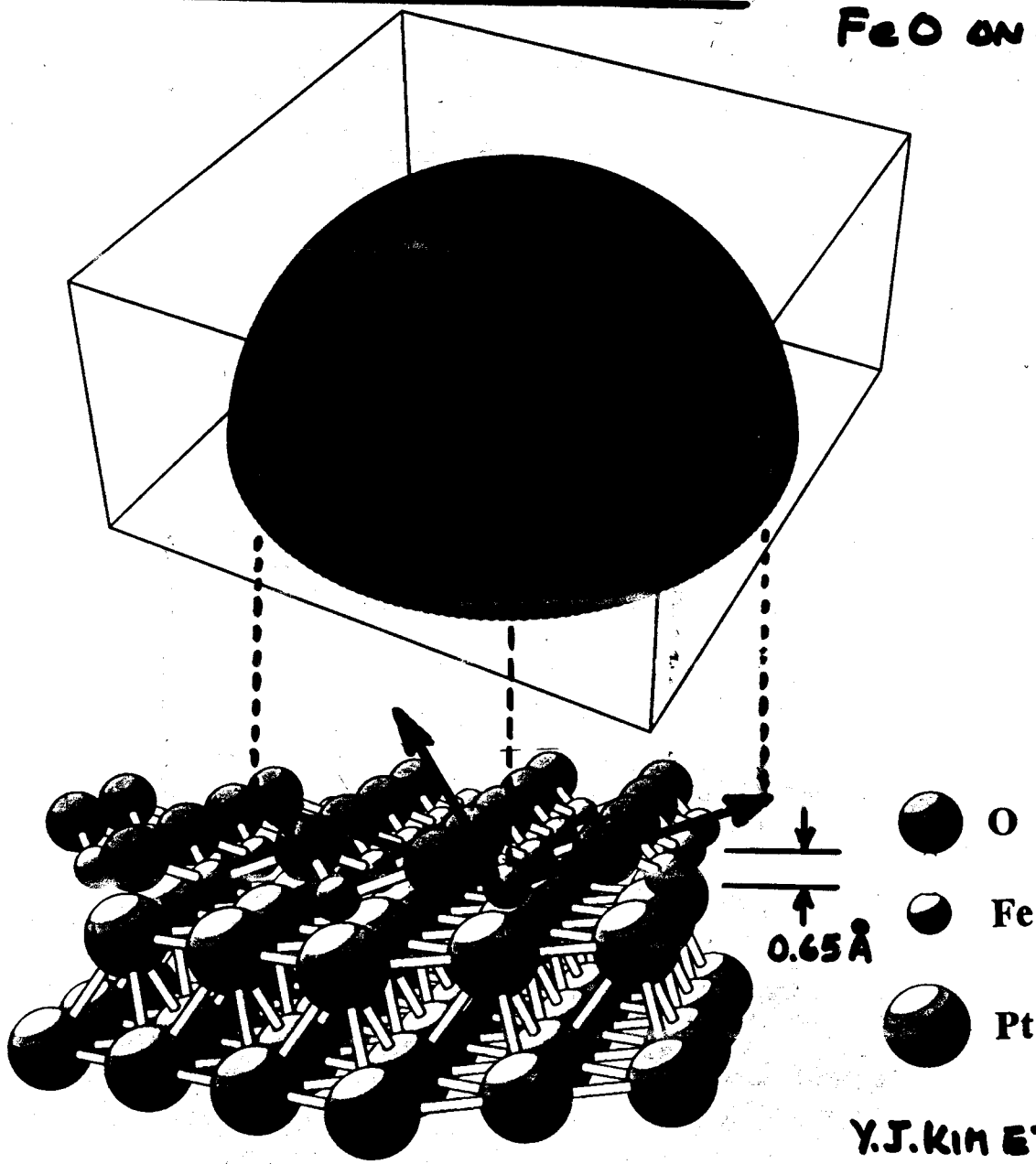


PHOTOELECTRON DIFFRACTION AND PHOTOCOMPARTMENT HOLOGRAPHY



- Element-specific and chemical state- or site-specific atomic structure
- Probes local or short-range order: long-range order not necessary (unlike LEED)
- Time-resolved measurements of surface reactions possible:
~10-20 s/spectrum now \rightarrow 0.1-1.0 s/spectrum with new detector and undulator
- Direct derivation of structural parameters from forward scattering and Fourier a/o holographic transforms of data
- Accurate structures ($\leq 0.05\text{\AA}$): expt. vs. multiple scattering theory with R-factors
- Variation of spin and light polarization for magnetic studies possible:
element-specific structure and magnetometry

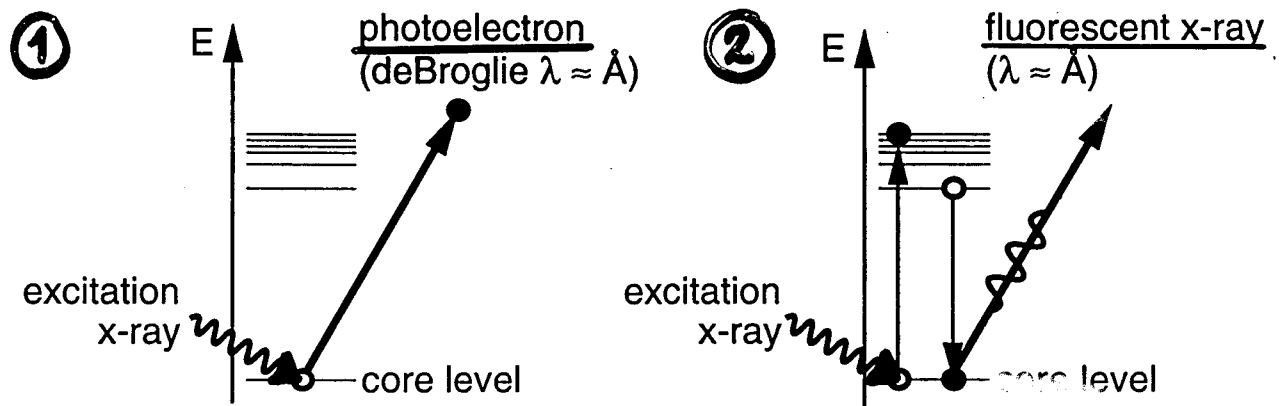
PHOTOELECTRON DIFFRACTION : Fe2p FROM
FeO ON Pt(111)



Y.J.KIM ET AL.,
PHYS. REV. B
55, R13448 ('97)

Atomic source holography (Szöke, 1986)

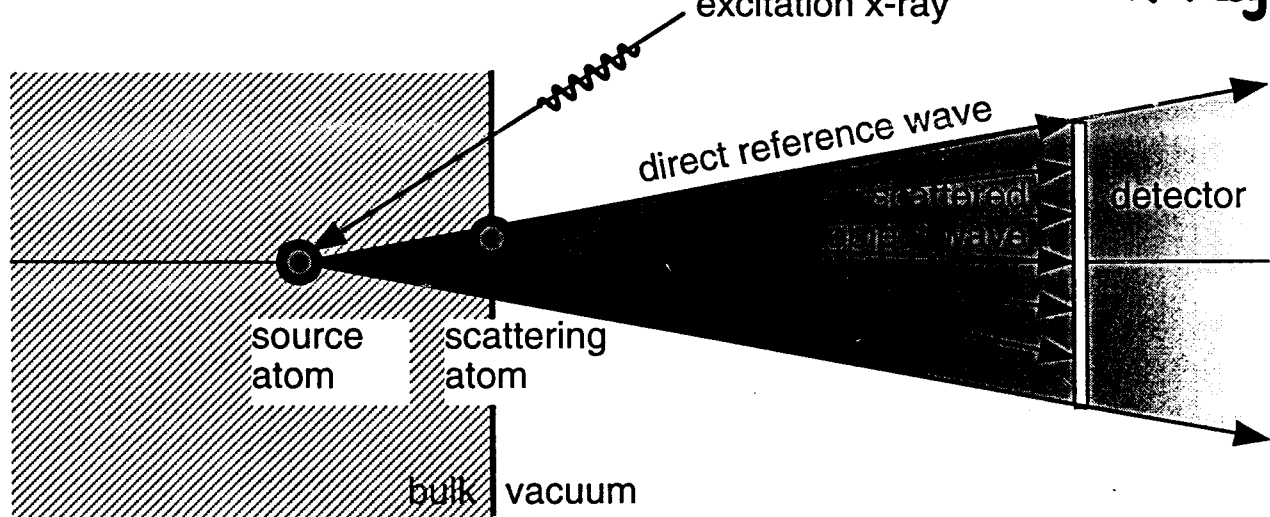
An atom can be photoexcited to emit a **photoelectron** or **fluorescent x-ray** wavefront.



③ δ -ray (+ resonant nuc. scatt.)

The interference between this **direct** electron or x-ray wavefront, and waves scattered by neighboring atoms creates a **hologram**.

④ Bremsstrahlung x-rays



Holograms can be collected for a range of wavelengths, "encoding" **spatial** information of the atomic **structure** surrounding the **emitter**.

How can **spatial** information of the **object** can be imaged from these **holograms**?

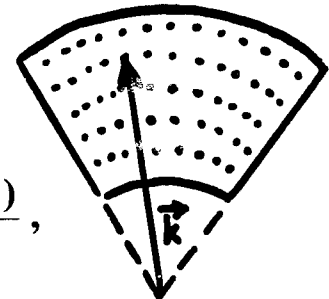
PHOTOELECTRON HOLOGRAPHY

+ X-RAY FLUORESCENCE HOLOGRAPHY

- Measure $I(\mathbf{k})$ at several directions of emission (several $\hat{\mathbf{k}}$), and several energies of excitation (several $|\mathbf{k}|$). \Rightarrow VOLUME IN $\vec{\mathbf{k}}$ -SPACE:

- Convert to normalized chi function:

$$\chi(\mathbf{k}) = \frac{I(\mathbf{k}) - I_0(\mathbf{k})}{I_0(\mathbf{k})} \text{ or } \frac{I(\mathbf{k}) - I_0(\mathbf{k})}{I_0(\mathbf{k})^{1/2}},$$



with $I_0(\mathbf{k})$ = intensity in the absence of scatterers.

- Holographically invert $\chi(\mathbf{k})$ via 3D transform (Barton, Tong et al.):

$$|U(r)| = \left| \int_{|\mathbf{k}|} \exp(-i|\mathbf{k}||\mathbf{r}|) \int_{\hat{\mathbf{k}}} \exp(i\mathbf{k} \cdot \mathbf{r}) \frac{\chi(\mathbf{k})}{F_j(\mathbf{k}, \mathbf{r})} |\mathbf{k}|^2 d|\mathbf{k}| \sin \theta_k d\theta_k d\phi_k \right|,$$

TWIN SUPPRESSION **ENERGY DIRECTION**

MULTI **SINGLE $h\nu$**

with: $\exp(-i|\mathbf{k}||\mathbf{r}|) \exp(i\mathbf{k} \cdot \mathbf{r})$ = kernel from single-scattering path-length-difference

θ_k and ϕ_k = angles defining direction of $\hat{\mathbf{k}}$.

W(110) Volume W 4f XPD

Angular data: 343 angles/energy, (90° sector) ~15 min/energy

Energy data: 58 energies total, $\Delta k = 0.1 \text{ \AA}^{-1}$, $h\nu = 73\text{-}333 \text{ eV}$

↳ ~20,000 data points

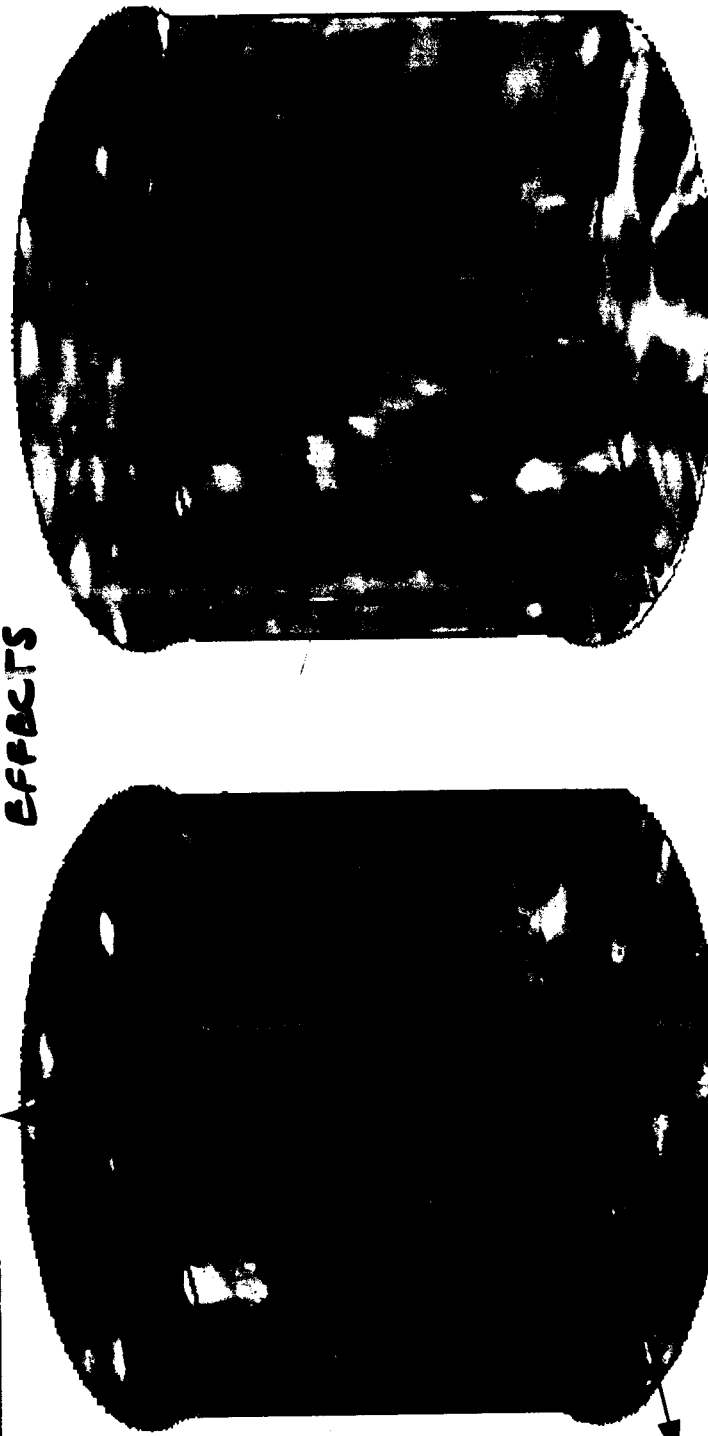
Bulk

[110]

$$\overline{k (\text{\AA}^{-1})} =$$

8.9

~30-50%
EFFECRS



Surface

$$\overline{KE} =$$

302

119

41

$$\theta_{\max} = 80^\circ$$

[111]

[001] 90°

35.3°

Comparison of experimental and theoretical images

W(110)-surface Emission

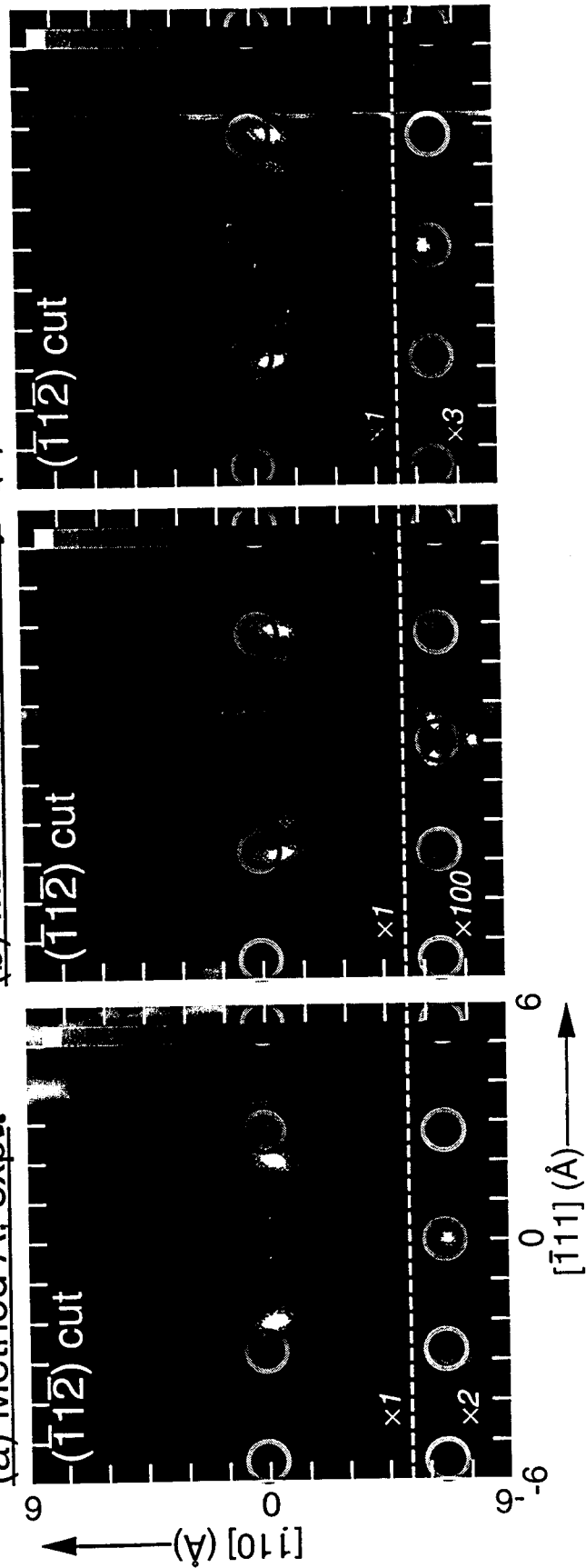
Method A

Barton, Tong et al.

$$K_A(\mathbf{k}, \mathbf{r}') = e^{i(\mathbf{k} \cdot \mathbf{r}' - kr')}$$

optical (Helmholtz-Kirchoff) kernel

(a) Method A, expt.



#Timmermans, Trammel, Hannoon, Appl Phys. 73, 6183 (1993) and Phys. Rev. Lett. 72, 832 (1994); Fadley, Sut. Sci. Reps. 19, 231 (1993); Kaduwela, Wang, Van Hove, Fadley, Phys. Rev. B, RC 50, 9656 (1994)

Sensitive to magnetic scatterers only,
but not to direction of scatterer spin,
simple phase behavior

= An image $U(r)$ from difference of spin-up and spin-down χ 's:

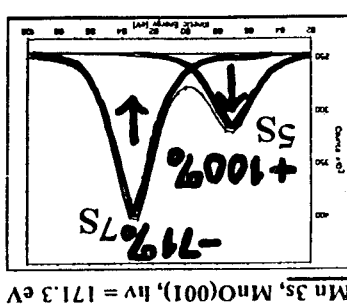
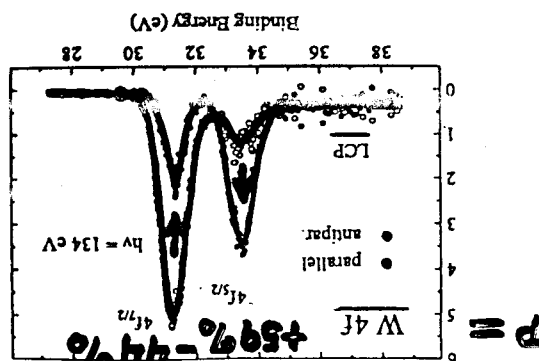
$$\Delta'(r) = \left| \int \exp(-i|\mathbf{k}||\mathbf{r}|) \int \exp(i\mathbf{k} \cdot \mathbf{r}) [\chi_\uparrow(\mathbf{k}) - \chi_\downarrow(\mathbf{k})] |\mathbf{k}|^2 d|\mathbf{k}| \sin \theta \mathbf{k} d\theta \mathbf{k} \right|^2$$

Sensitive to magnetic scatterers only
and direction of scatterer spin,
complex phase behavior

$\Delta(r) = U_\uparrow(r) - U_\downarrow(r)$ = Difference of spin-up and spin-down images $U(r)$:

• Holographically invert with two spin-sensitive transforms:

• Convert to χ_\uparrow and χ_\downarrow .



and/or

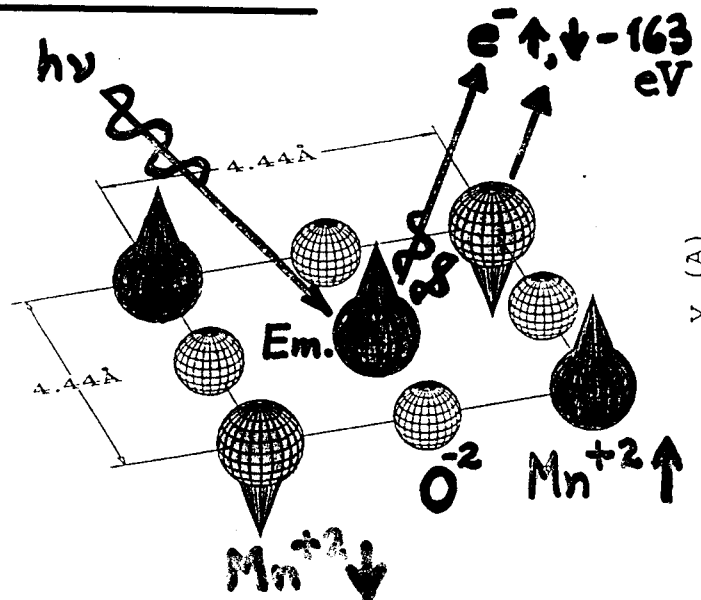
—multiple-split peaks:

• Measure $I_\downarrow(k)$ and $I_\uparrow(k)$ at ~equal energy via:

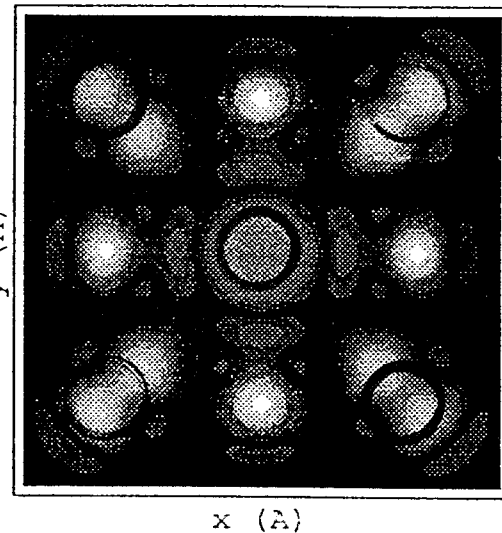
-----SPIN-POLARIZED PHOTOELECTRON HОLOGRAPHY-----

DIRECT IMAGING OF MAGNETIC ATOMS WITH SPIN-POLARIZED PHOTOELECTRON HOLOGRAPHY?

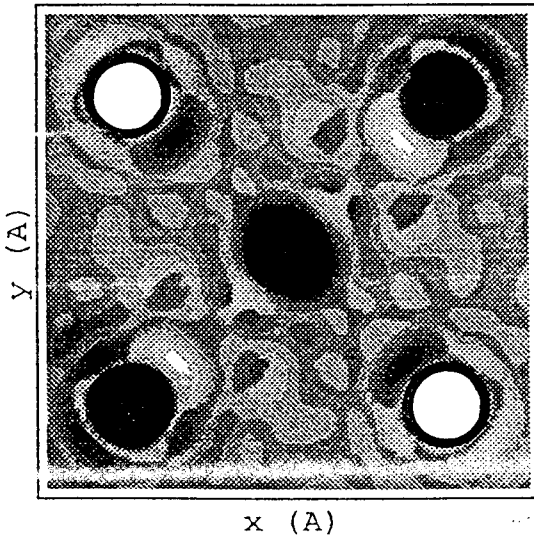
SIDE SCATTERING:



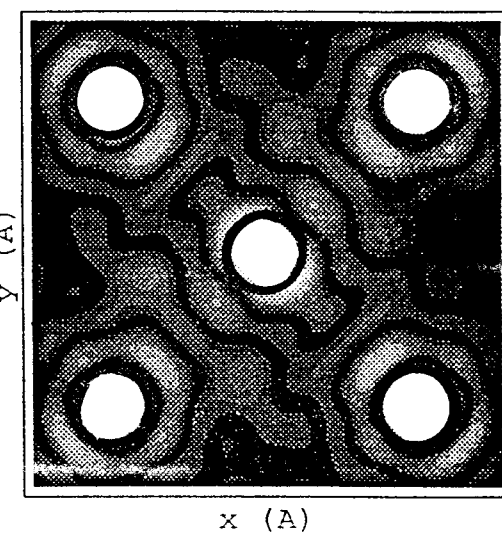
Model cluster of MnO



Normal image: $U_p = |\text{F.T. of } \chi|$,
Positions of all atoms

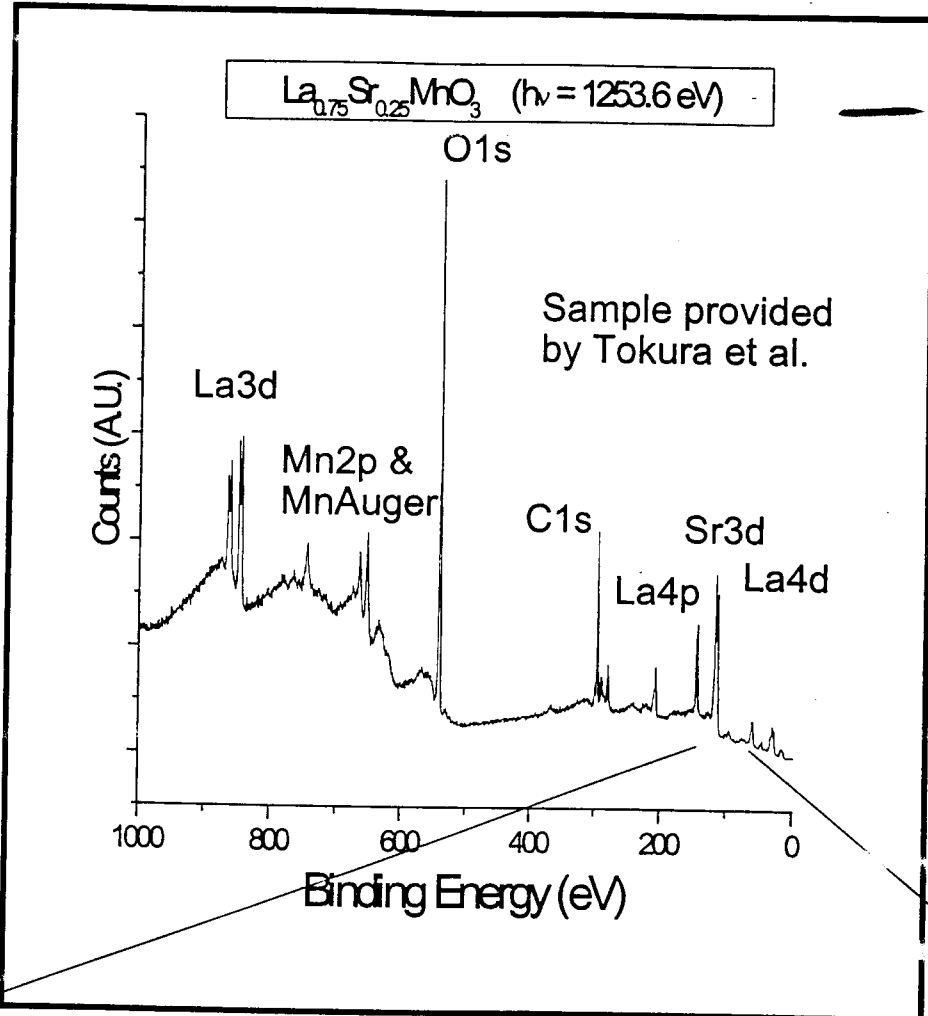


Spin-sensitive image: $\Delta =$
Spin orientations of $U_p - U_d$
magnetic atoms



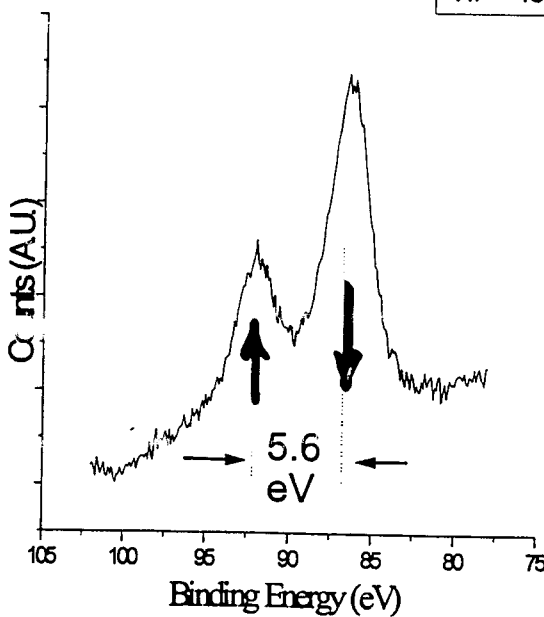
WANG,
KADUWELA
ET AL.,
P.R.B 50,
29656 (1994)

FIRST
DATA
FOR A
CRM
SAMPLE



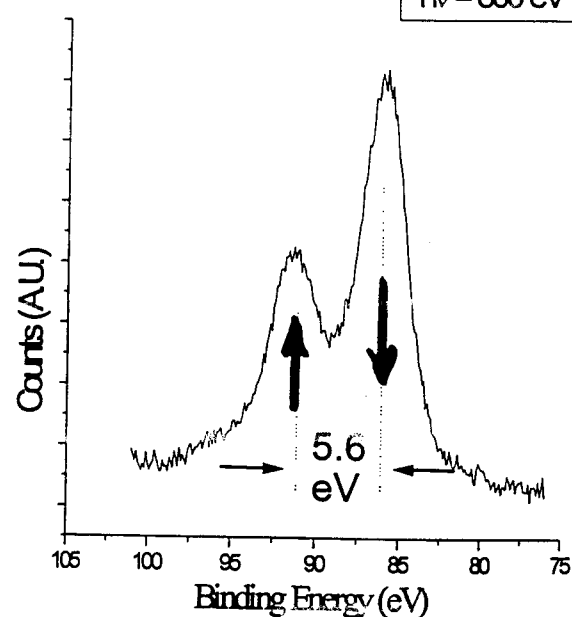
Mn3s

$h\nu = 400 \text{ eV}$

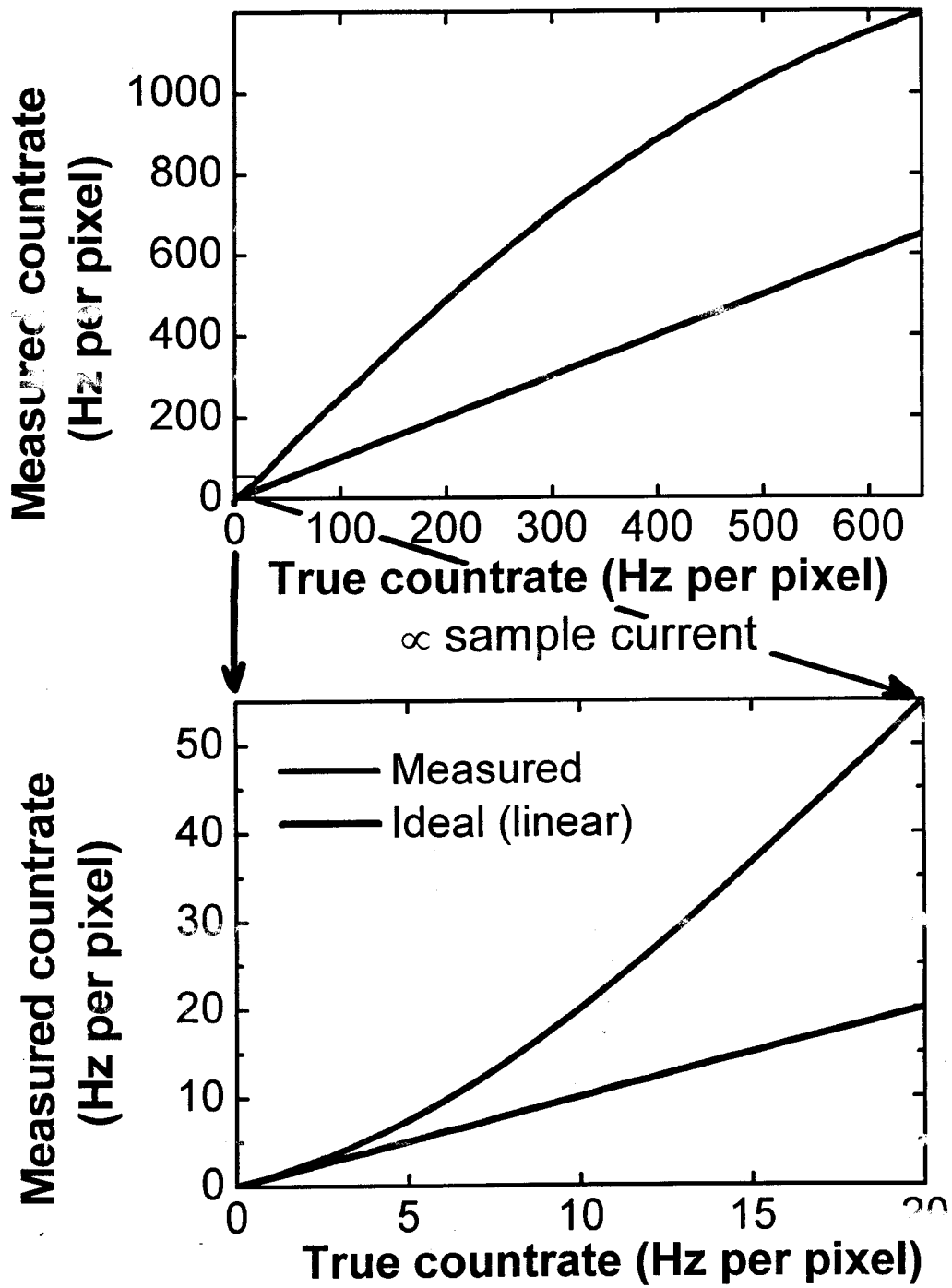


Mn3s

$h\nu = 800 \text{ eV}$

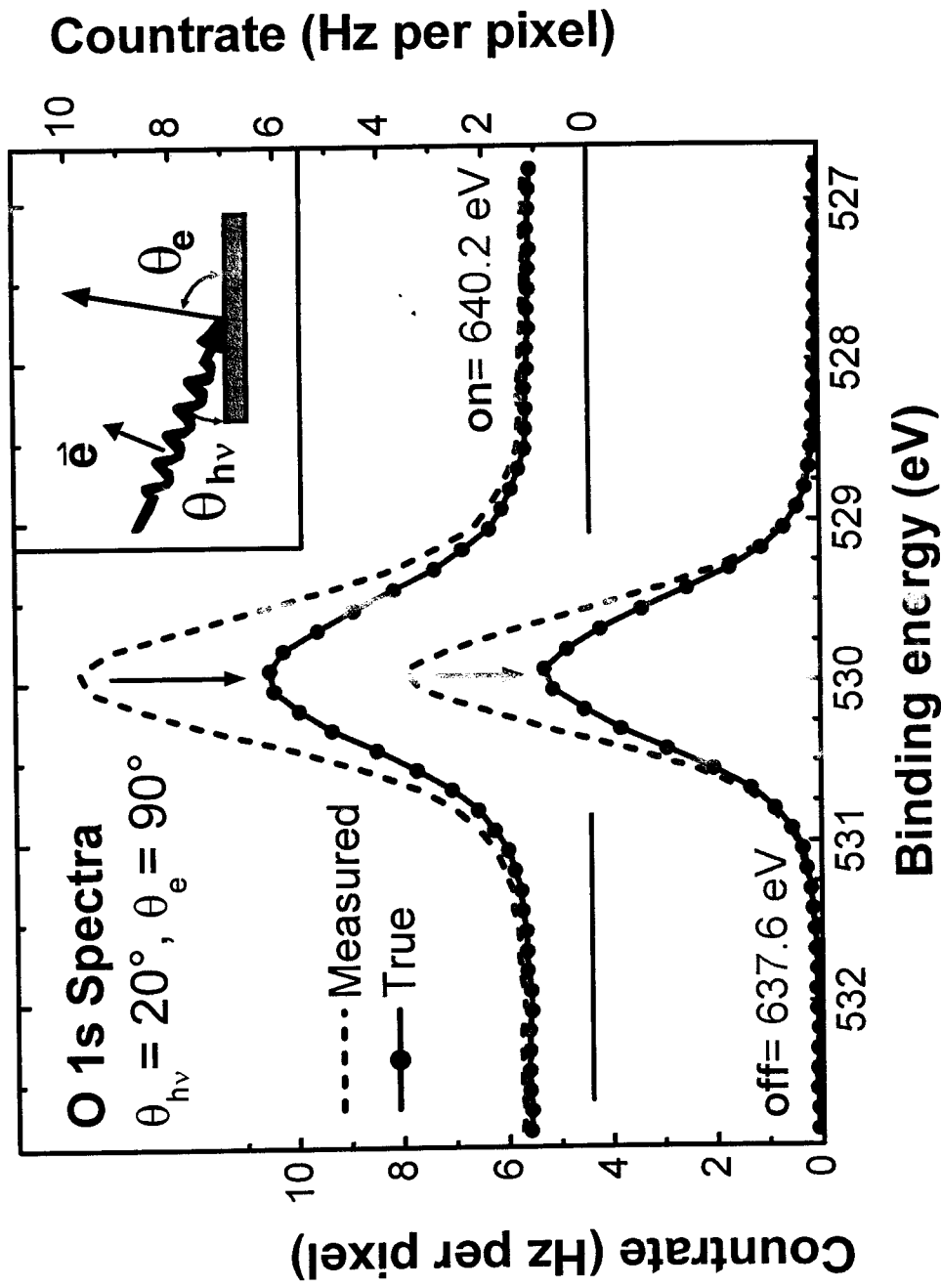


Scientia ES200 - Detector Response*

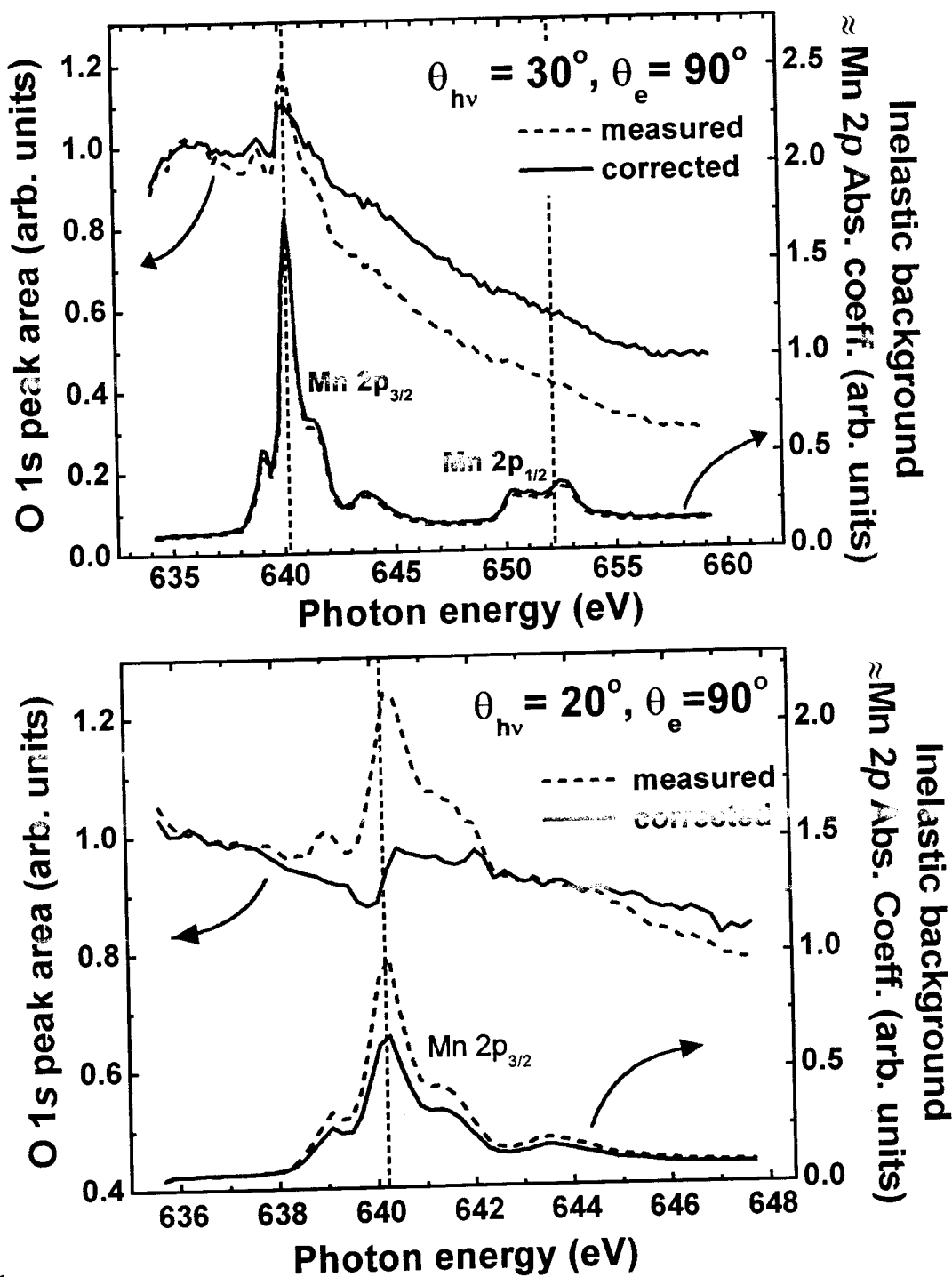


* As set up
by mfr.

Correction of Individual Spectra O 1s on/off Mn 2p resonance



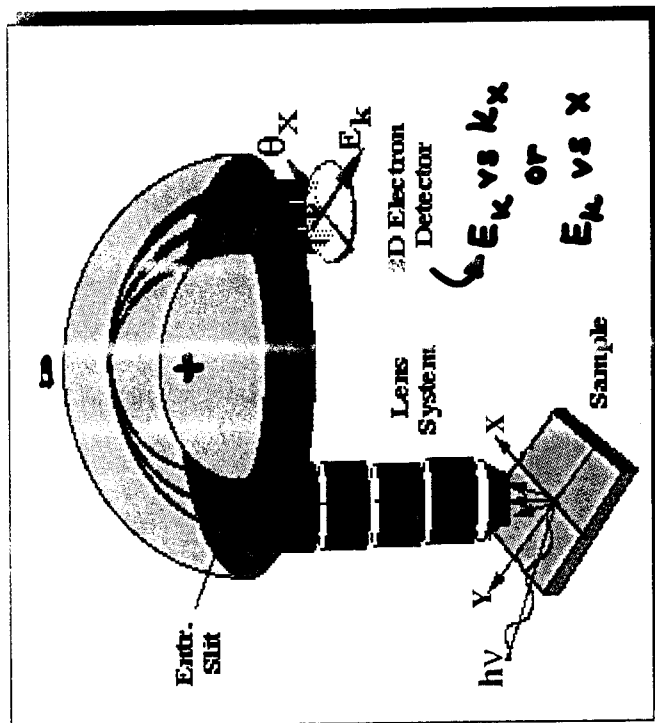
Measured and Corrected Results



Angle-Resolved Photoemission Spectroscopy (ARPES)



Advanced Light Source



Scienta SES-200

High Energy Resolution (2meV);

High Momentum Resolution (0.2° in Angular Mode);

Parallel Angle Collection of $\sim 14^\circ$.

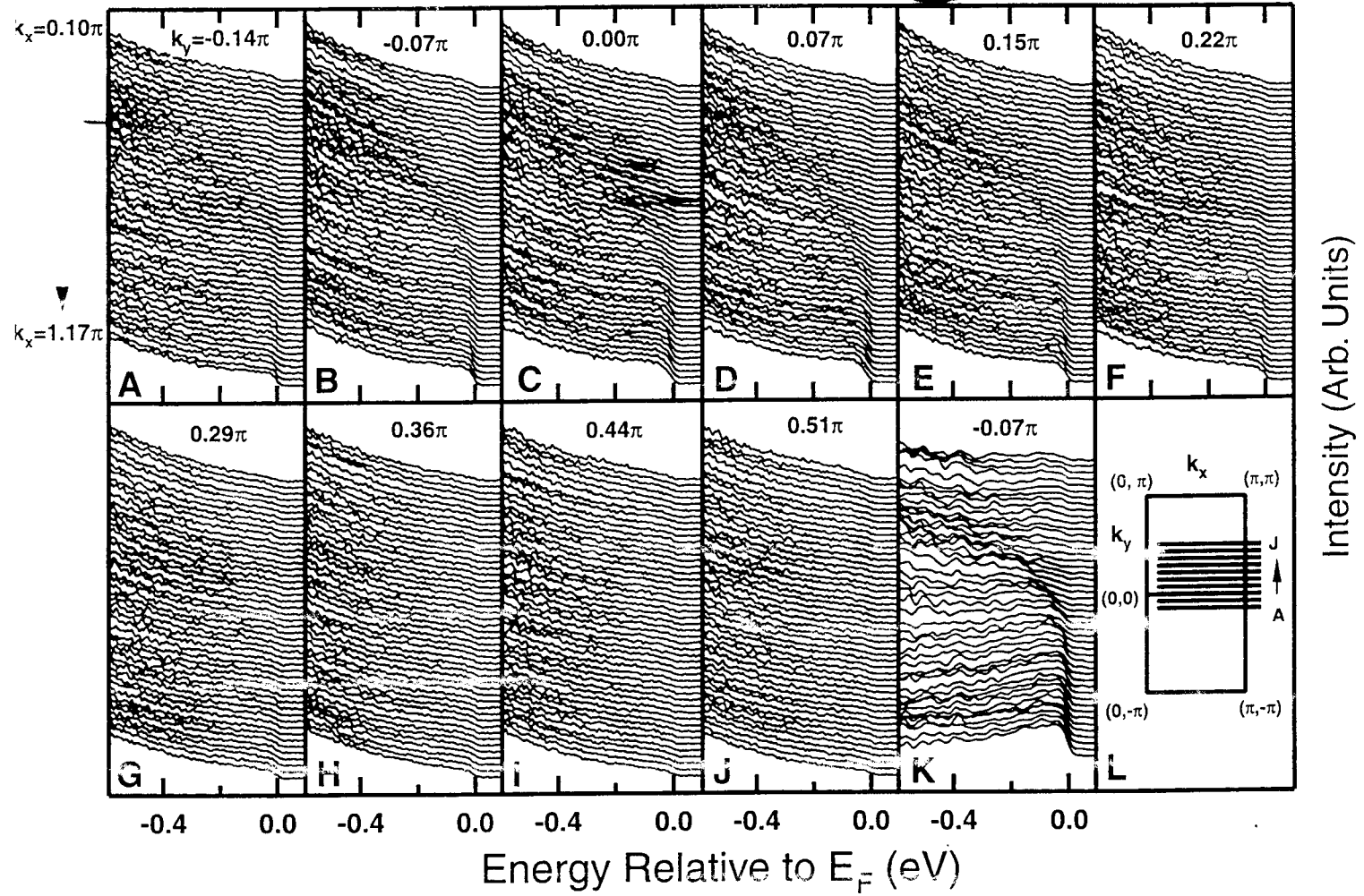


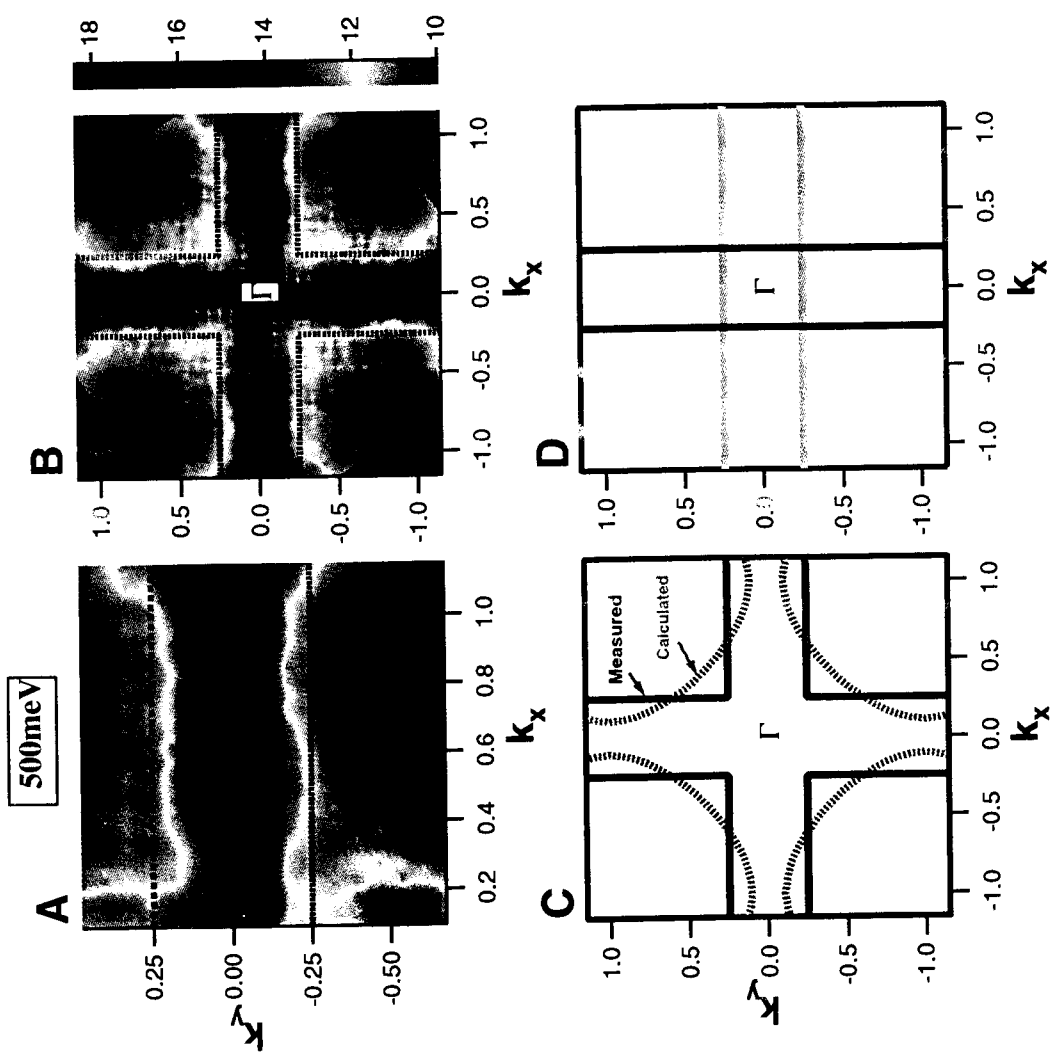
Fig. 1. Angle-resolved photoemission spectra taken on Nd-LSCO at 20 K. The measurement scheme is depicted in (L), which covers the first and fourth quadrants. Each of the panels (A) to (j) represents a cut parallel to the (0,0) to (π ,0) direction with k_x covering from 0.10π to 1.17π with an interval of 0.023π . (A) to (j) cover k_y from -0.14π to 0.51π with an interval of 0.07π . (K) shows the same spectra as in (B), but with the high-energy background removed.

ZHOU ET AL.,
SCIENCE
286, 268 (2000)



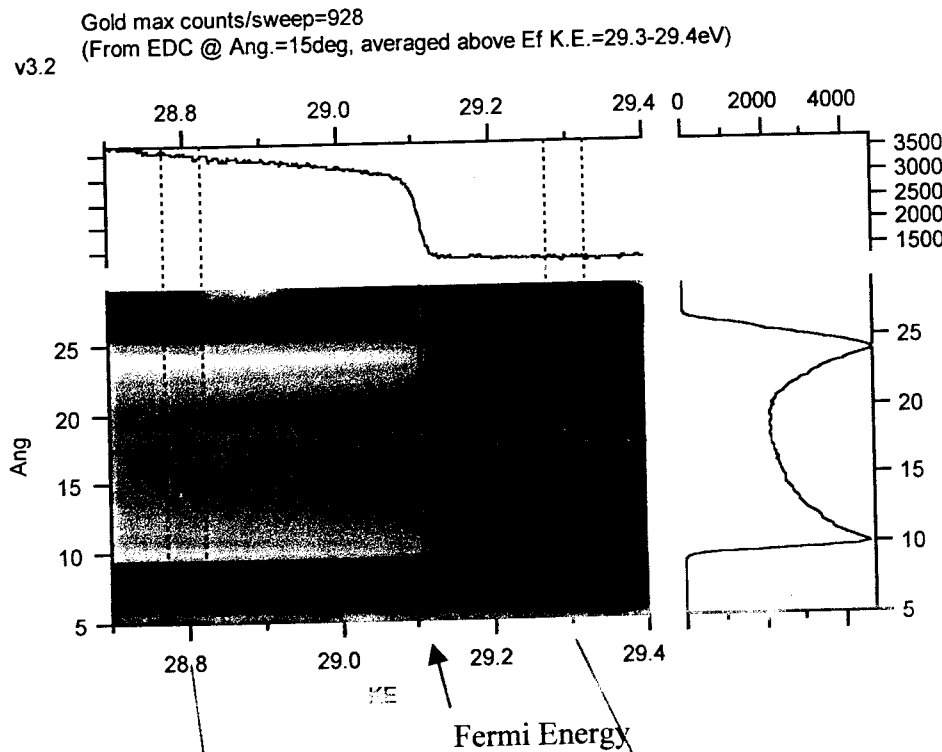
$n(k)$ and Fermi Surface for Nd-LSCO

Advanced Light Source

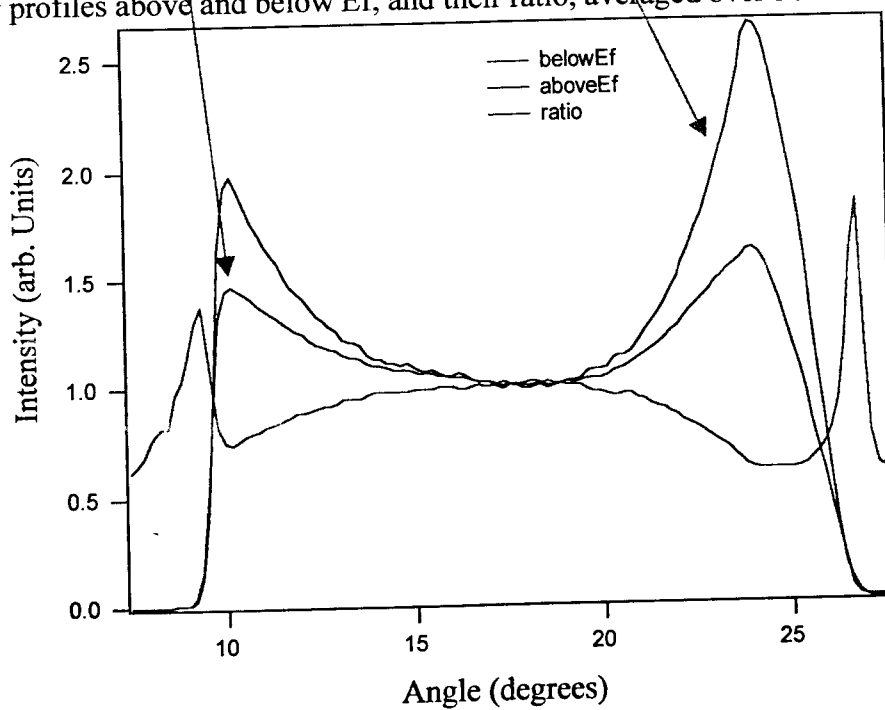


Scienta Detector Nonlinear Response Determined from Gold Study

Exemplary Scienta angle-mode scan
polycrystalline Gold, ALS BL 10.0.1 $h\nu=33\text{eV}$



Angular profiles above and below Ef, and their ratio, averaged over 50meV energy window



* Intensity profile from second-order light emission should match 1st Harmonic emission profile! The difference here is count rate.

**GROMKO,
LI, FEDEROV,
DESSAU**

**TIME-RESOLVED SPECTROSCOPY
AT THE ADVANCED LIGHT SOURCE:**

OR ELETTRA OR ...

Photoelectron spectroscopy/diffraction/holography:

-Undulator beamline (U5)

$$\rightarrow \sim 5 \times 10^{12}$$

----> 10^{13} photons/sec into

$$1:10^3 < \begin{cases} 0.1 \text{ eV} @ 100 \text{ eV} \\ 1.0 \text{ eV} @ 1000 \text{ eV} \end{cases}$$

-Advanced photoelectron spectrometer with $\pm 6^\circ$ acceptance and 100-700 channel high-speed detector

----> full spectrum at one time

-Overall photon-to-detected e⁻ yield of 10^{-4} - 10^{-6} for single spectral peak (e.g., C 1s, Fe 2p)

----> 10^7 - 10^9 electrons/sec over peak

-For 1% statistics in 100-channel spectrum

----> spectrum in 10^{-1} - 10^{-3} sec

Prototype Next-Generation Multichannel Detector

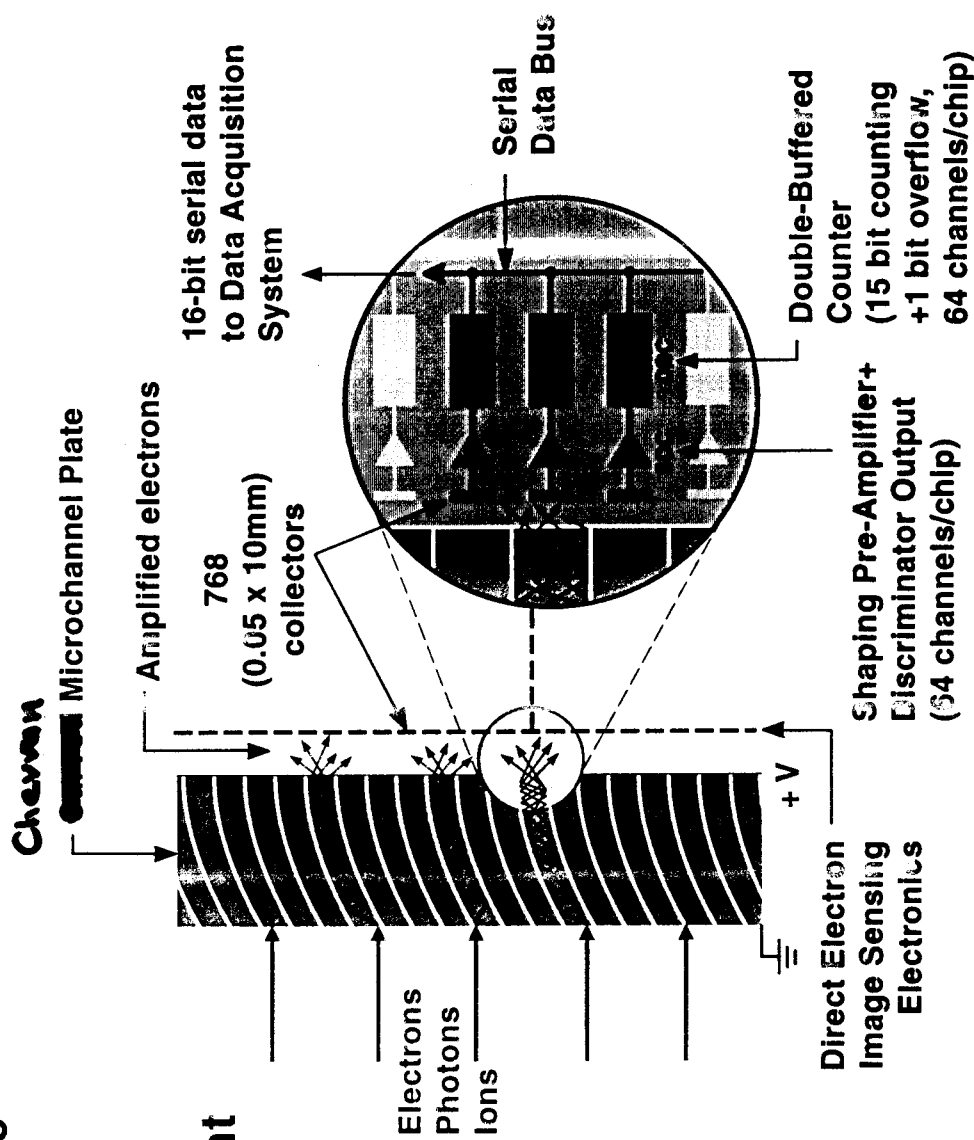
- 10^9 /second overall counting rate

- $12 \times 64 = 768$ channels with
0.050 mm = 50 micron = 0.002" spacing and 10 mm = 0.4" height

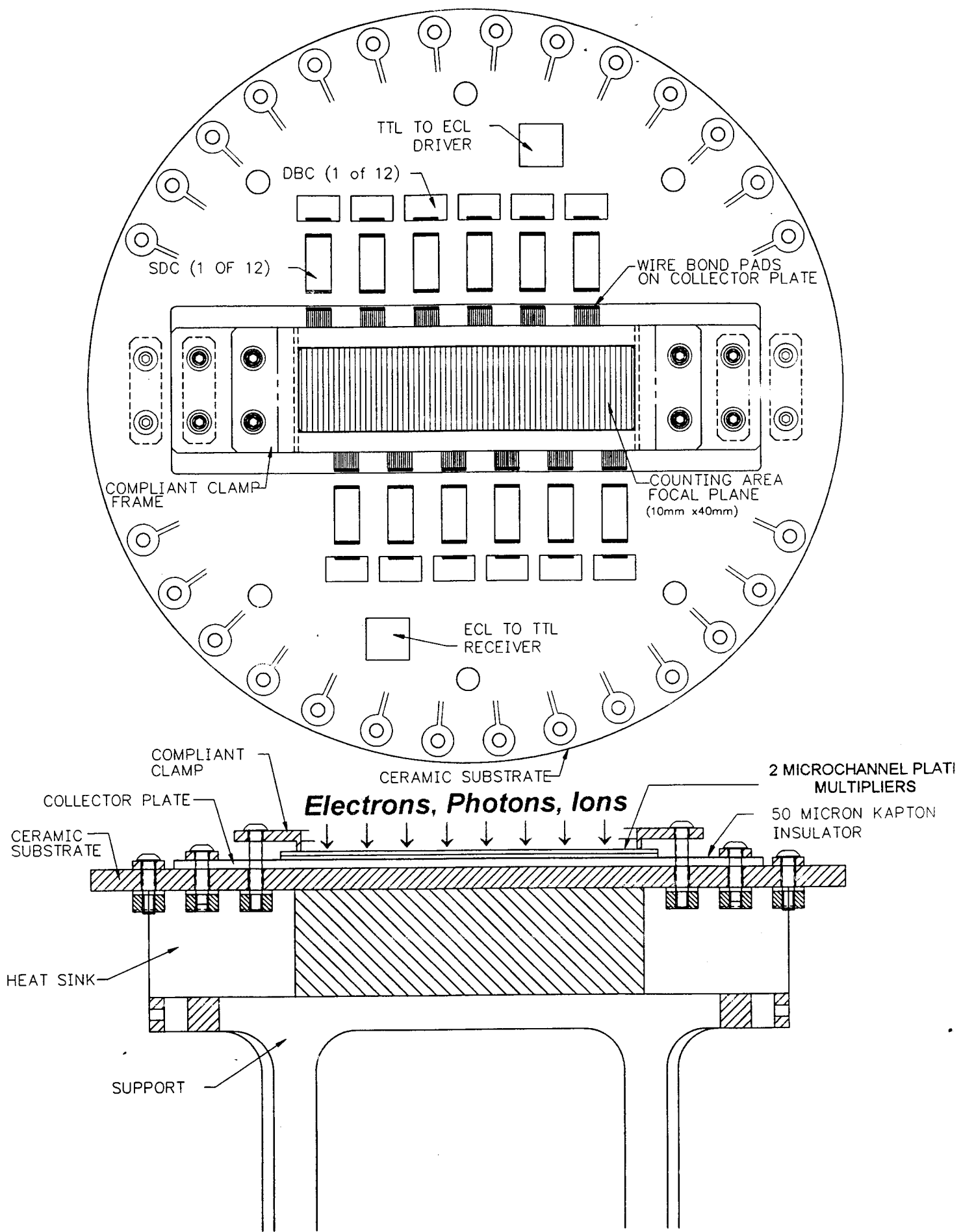
- Application-specific
64-channel integrated
circuits:

- pre-amplifier ("SDC"):
from high-energy physics
- counter ("DBC"):
custom-designed

- Now undergoing first
successful tests with
photon counting
and electron



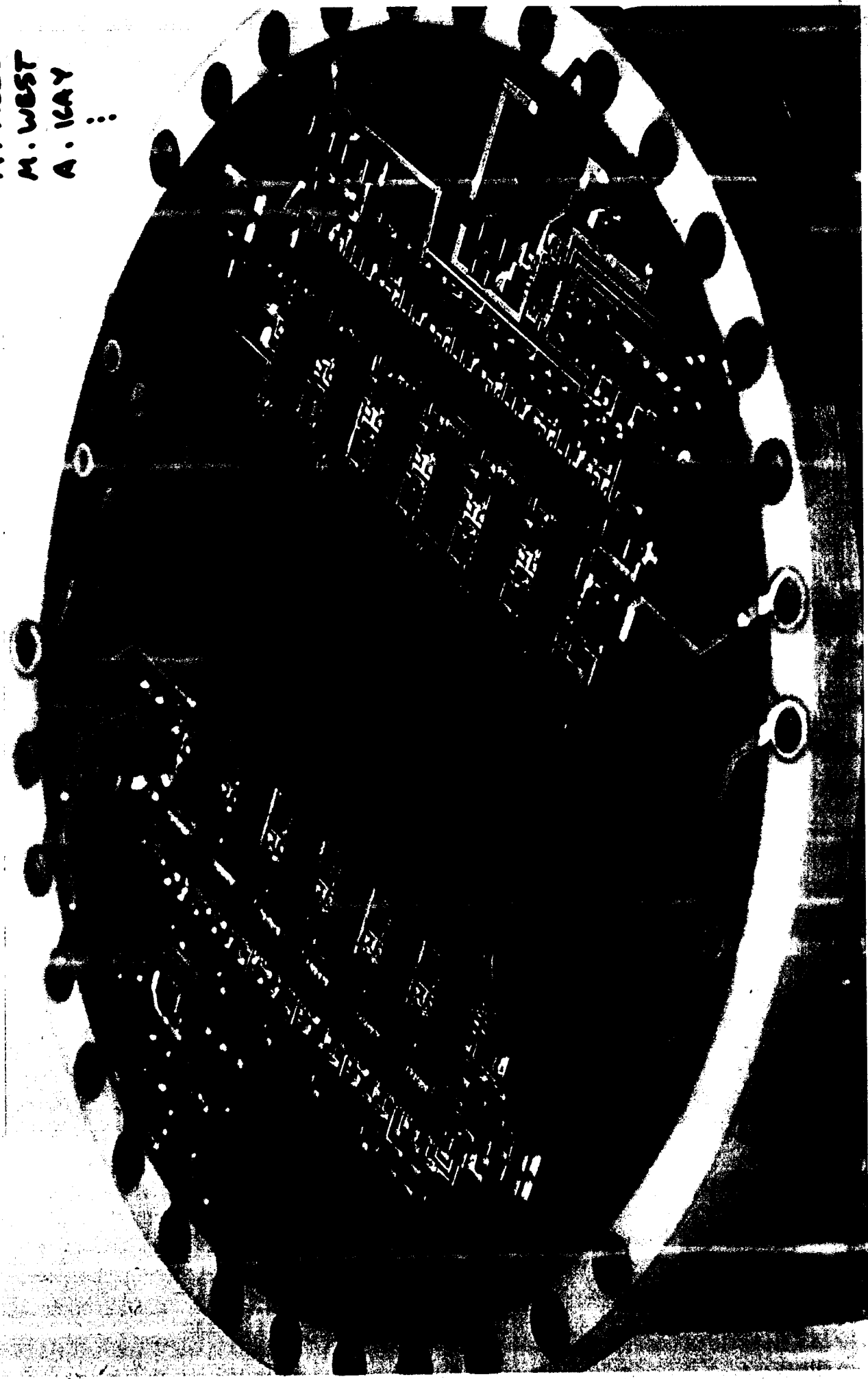
Overall detector layout



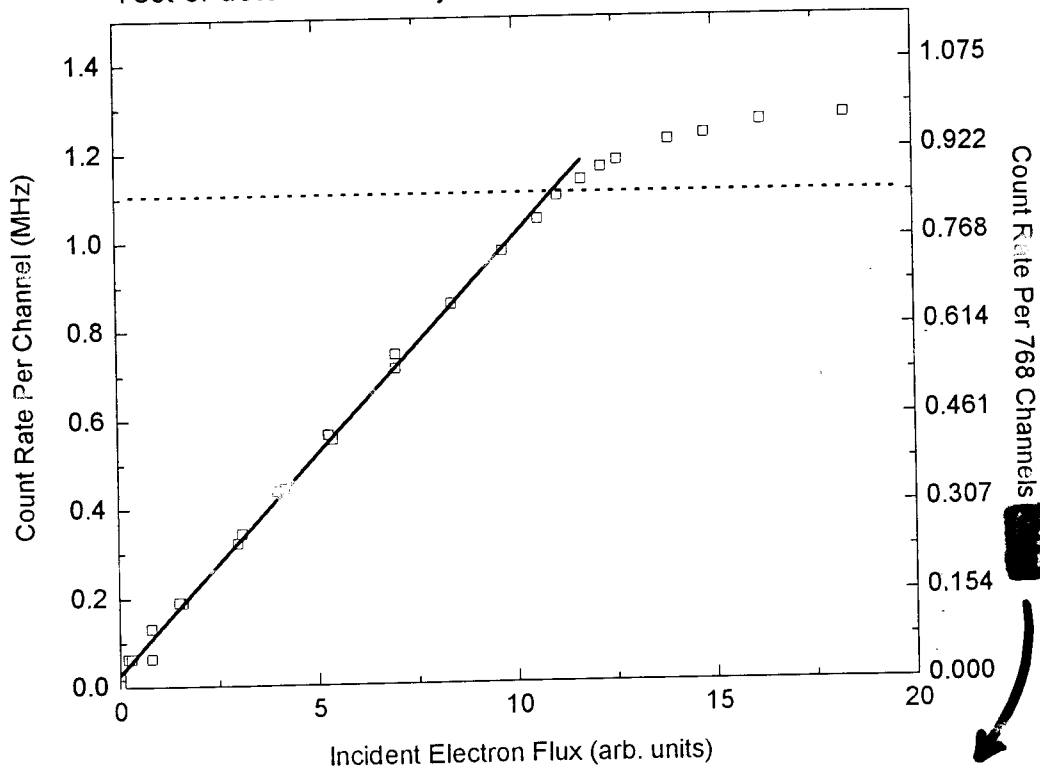
A NEXT-GENERATION
MULTICHANNEL DETECTOR

768 channels, 50 micron spacing, 1 GHz overall

J. KATZ
B. TURNER
M. PRESS
M. WEST
A. ICAY



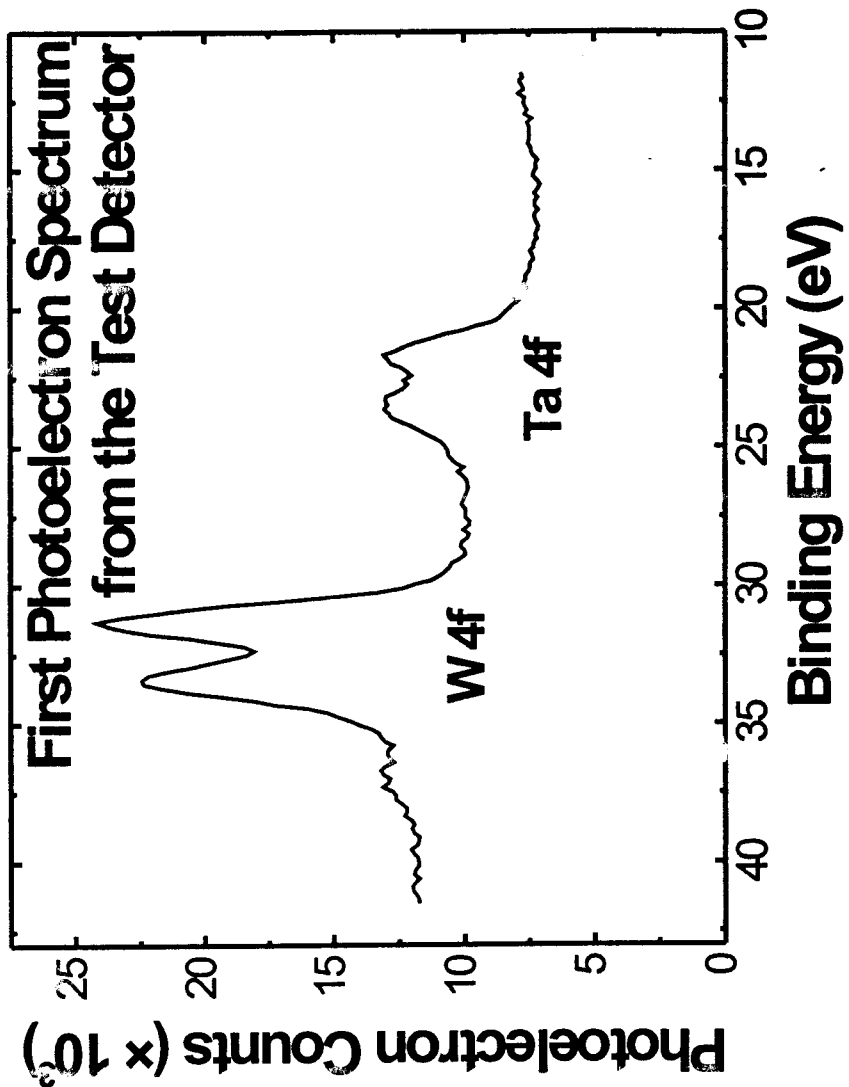
Test of detector linearity - electron flood gun



SPECTRA
100 - 1000 TIMES
FASTER,
DOWN TO msec
RANGE

High Speed Detectors for Use at the ALS

FEASIBILITY TEST: FIRST SPECTRA AT THE ALS



- Test detector in actual UHV environment
- Test sample: tungsten+tantalum

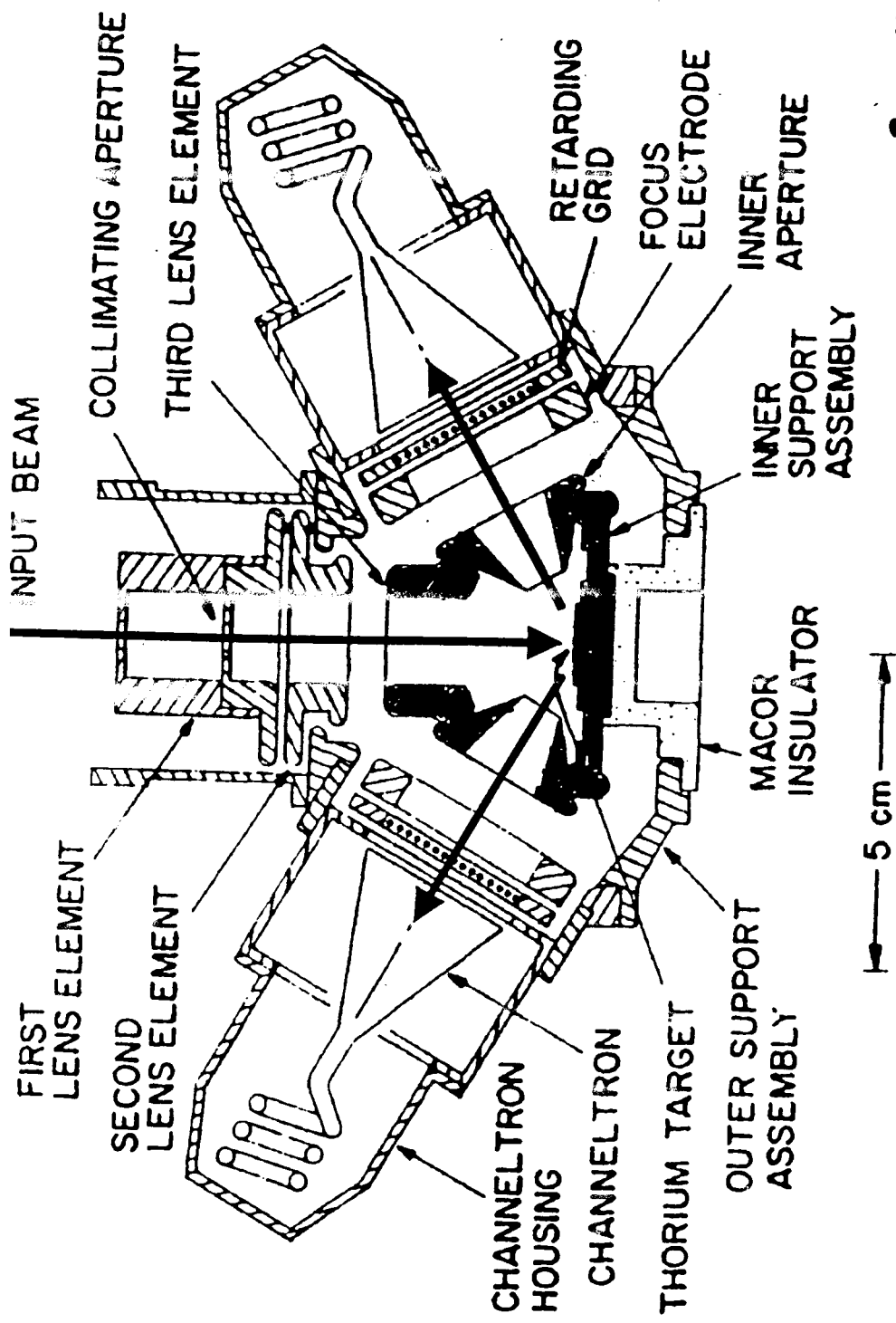
Comparison of several existing detectors:

Detector	Channel Width, Δr (μm) [1]	Resolution $= \Delta E/E_{\text{pass}}$ $\times 10^{-4}$ [2]	Number of Channels	Maximum Count Rate Per Channel	Maximum Overall Count Rate [3]
-ONE-DIMENSIONAL:					
ELETTRA Project (Italy)–MCP + ex situ IC's [4]	320	8.0	96	5 MHz	5 MHz [5]
Integrated Sensors, Inc.–MCP + single wafer IC's (UK)	160	4.0	116	100 kHz	12 MHz
BNL Highspeed—MCP + on-board IC's: 1 st generation (2 nd generation—this proposal)	50 (50)	1.3 (1.3)	768 (768)	~1.1 MHz (>2 MHz)	0.8 GHz (>1.6 GHz)
PHI MultiChannel (US)—multiple channeltrons	2000	50.0	16	~1 MHz	~16 MHz
-TWO-DIMENSIONAL:					
Quantar—MCP + Resistive Anode (US) [6]	155 400	3.9 10.0	256 100	300 kHz 1 MHz	300 kHz 1 MHz
Scienta MCP + CCD, in greyscale mode (Sweden)	110	2.8	~367	< 2 kHz	< 750 kHz--non-linearity

Table 1—Performance characteristics of the existing one-dimensional and two-dimensional detectors for electrons and soft x-rays

- [1] Channel width not including channel crosstalk effects. The LBNL detector has a $75\mu\text{m}$ effective width including this crosstalk (cf. Fig. 1(e)), still smaller than the non-corrected figures for all other detectors.
- [2] Resolving power is computed from the effective channel width, applied to the case of a 200mm hemispherical electron analyzer (Scienta ES200). In this case, with $E_{\text{pass}} = \text{pass energy after retardation}$ and $r_0 = \text{mean analyzer radius}$, $\Delta E/E_{\text{pass}} = \Delta r/2r_0$. Note that the best possible resolving power for the Scienta ES200 is $\Delta E/E_{\text{pass}} = 10^3$.
- [3] This figure represents all channels running at near saturation. In practice, the detector would generally be used to collect signals that vary in intensity across the dispersion axis (i.e. spectral features). This results in some channels perhaps running near saturation, but others significantly below the saturation level. In such cases, this overall actual count rate will not be as high as stated.
- [4] Non-commercial development project at the ELETTRA synchrotron radiation facility in Trieste, with first description in L. Gori, et al., Nuc. Instr. and Meth. A, 431 (1999) 338-346.
- [5] Overall-detector linear count rates actually achieved to date, including combined limitations due to electron multiplier, preamp+counting electronics, and external data handling system. Thus, the final column is not always equal to the product of the two next to it.
- [6] Figures for two different Quantar models are given. The per-channel and global count rates are always identical due to the nature of the detector.

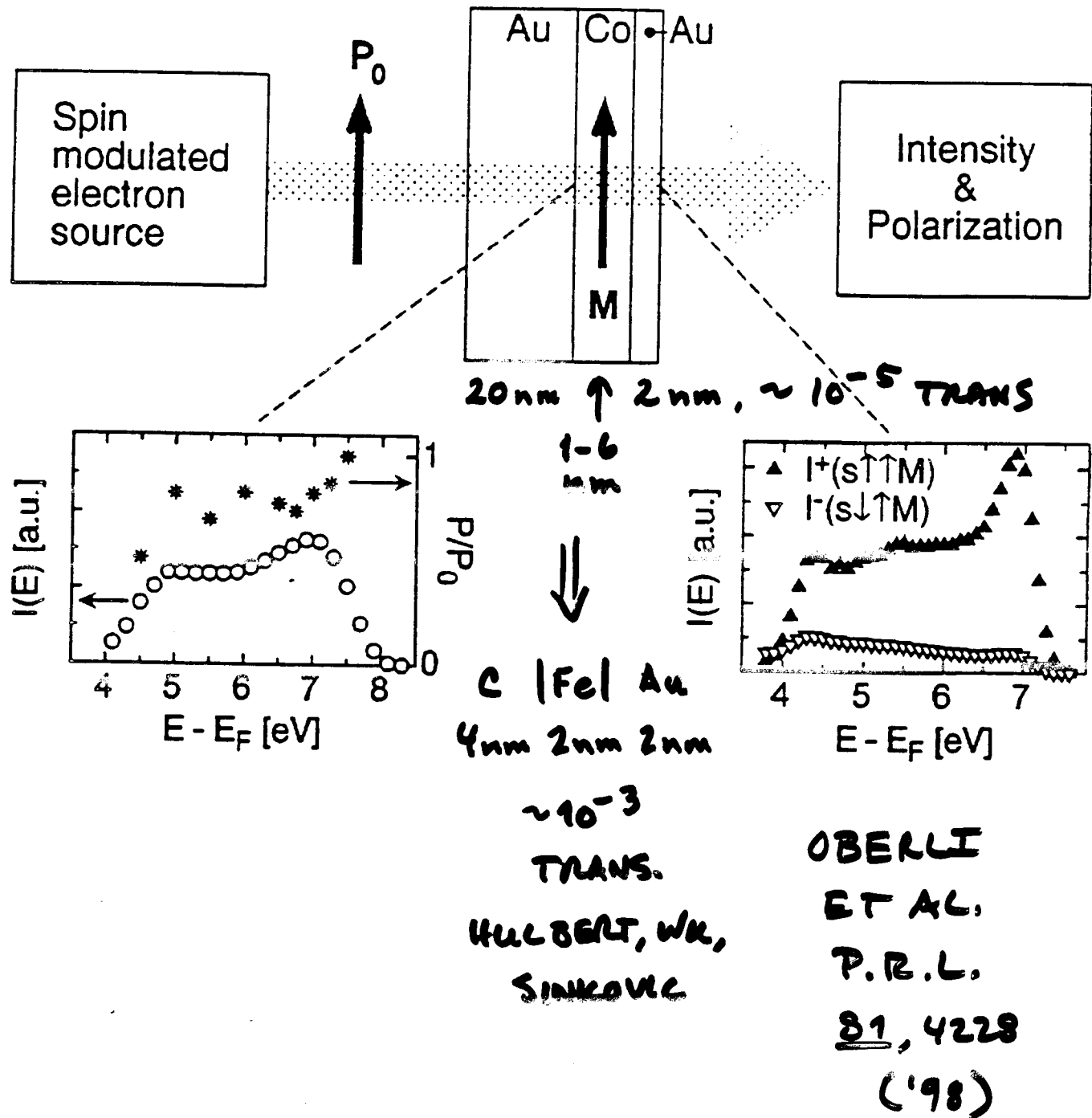
THE MICERONOTT SPIN DETECTOR



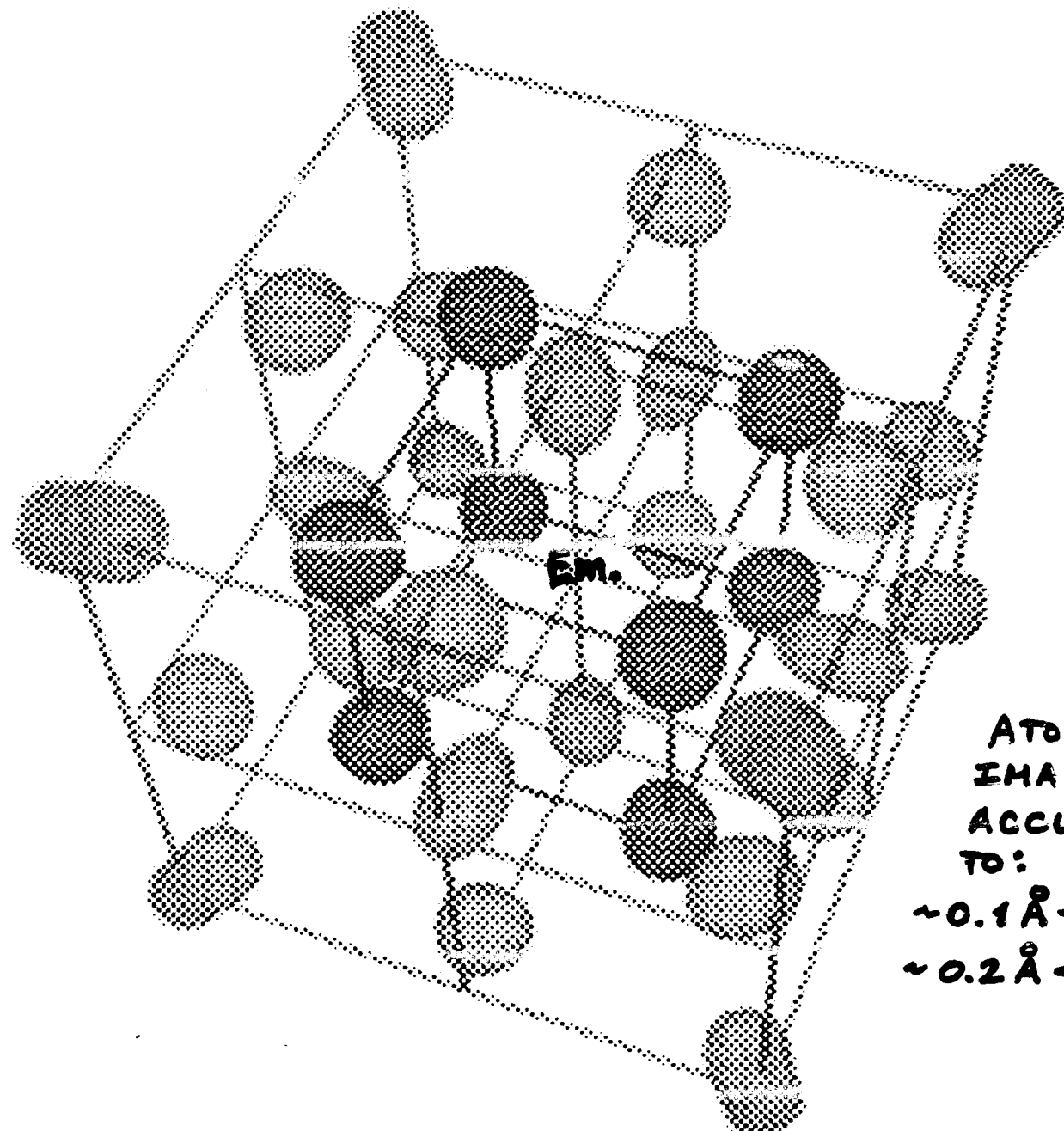
Design: B. Dunning, Rice Univ., Houston, TX

$\sim 10^{-3} - 10^{-4}$
EFFICIENCY

THE SPIN FILTER?



Fe XFH - TWO E's : FeK α , FeK β
6.38 keV, 7.08 keV



ATOMIC
IMAGES
ACCURATE
TO:
~0.1 Å - NEAREST
~0.2 Å - FURTHER
AWAY

HIOERT ET AL.
(MATERLIK GROUP)
PHYS. REV. B,
S1, R830 ('00)



Holographic Imaging with X-rays

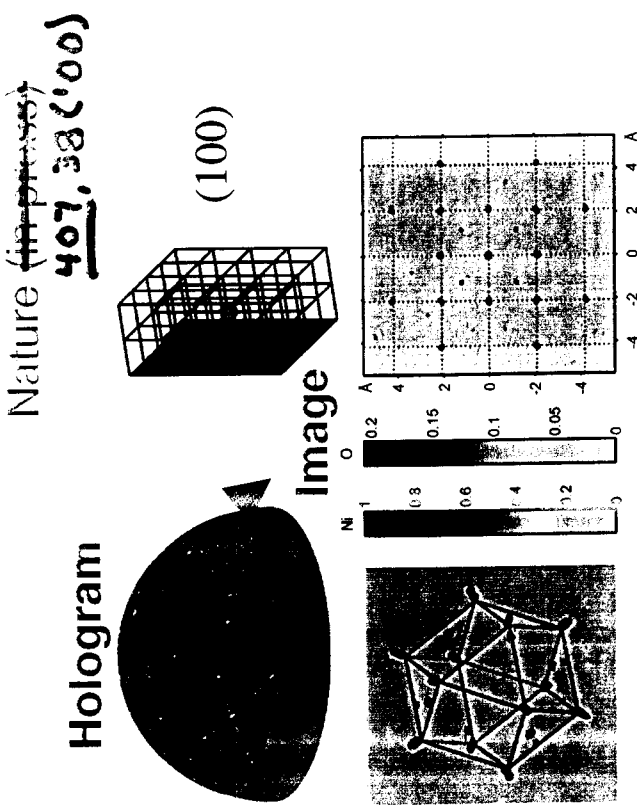
X-RAY FLUORENCE HОLOGRAPHY

--RECENT RESULTS--

With 3rd generation light source, low-Z eleme nts become visible:

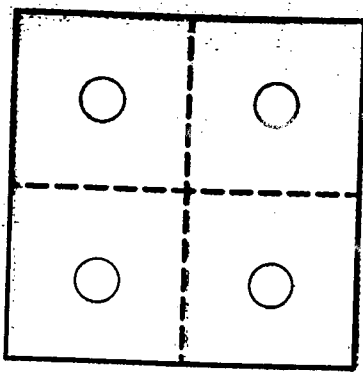
- O around Ni in NiO
 - ~150 O and Ni atoms imaged
 - neighbours around Mn in MnAlPd
 - average atomic distribution image

Image
Hologram
Nature (http://dx.doi.org/10.1038/nature03389)
401, 38 (2000)



Ge Fluorescence Detector and Electronics Development for Attitude XAFS

- Expertise in nuclear counting to XAFS detectors
- Detector group at LBNL
- Novel and efficient design
- Simple to use, quiet, and rugged
- 12-element detector



Back Contacts

-600 V

\Rightarrow 1 MHz
over
dead
time

Monolithic Ge 2x 2 cm

*Electrically divided into four-pixels
No physical separation of pixels
Amorphous Si coated*